frontiers | Frontiers in Earth Science

TYPE Original Research
PUBLISHED 19 January 2023
DOI 10.3389/feart.2023.1123633

OPEN ACCESS

EDITED BY
Xiaoyu Guo,
Sun Yat-Sen University, China

REVIEWED BY
Wei Li,
China University of Geosciences Wuhan, China
Yun Chen,
Institute of Geology and Geophysics (CAS), China
Jikun Feng,
University of Science and Technology of China, China
Xuzhang Shen,
Sun Yat-Sen University, China

*CORRESPONDENCE
Xinlei Sun,
xsun@cdut.edu.cn

SPECIALTY SECTION
This article was submitted to Solid Earth Geophysics, a section of the journal Frontiers in Earth Science

RECEIVED 14 December 2022
ACCEPTED 10 January 2023
PUBLISHED 19 January 2023

CITATION
Xiao Z, Sun X, Yang J and Gao Y (2023), Dense-array adjoint tomography reveals lithospheric delamination and asthenosphere upwelling beneath the western Yangtze Craton.
Front. Earth Sci. 11:1123633.
doi: 10.3389/feart.2023.1123633

Dense-array adjoint tomography reveals lithospheric delamination and asthenosphere upwelling beneath the western Yangtze Craton

Zhuo Xiao[1,2], Xinlei Sun[3]*, Jianfeng Yang[4] and Yuan Gao[5]

[1]CAS Key Laboratory of Ocean and Marginal Sea Geology, South China Sea Institute of Oceanology, Guangzhou, China, [2]Southern Marine Science and Engineering Guangdong Laboratory (Guangzhou), Guangzhou, China, [3]International Center for Planetary Science, College of Geosciences, Chengdu University of Technology, Chengdu, China, [4]State Key Laboratory of Lithospheric Evolution, Institute of Geology and Geophysics, Chinese Academy of Sciences, Beijing, China, [5]Key Laboratory of Earthquake Prediction, Institute of Earthquake Forecasting, China Earthquake Administration, Beijing, China

The eastern Tibetan Plateau has attracted widespread attention due to its complex topography and strong seismicity. However, the mechanism controlling the growth of this margin remains enigmatic. Here, we present detailed upper mantle structures of the easternmost and northeastern Tibetan Plateau from dense-array adjoint waveform tomography. The seismic images show mushroom-shaped low-velocity zones atop at the uppermost mantle of the eastern margin of the Tibetan Plateau and slab-shaped high-velocity bodies preserved beneath both the eastern Himalayan syntaxis and the western Sichuan basin. The seismic features suggest asthenosphere upwelling and lithospheric delamination beneath the western Yangtze Craton, which might be induced by the retreat of the subducted Indian Plate. Our study shows that the mantle dynamics of the western Yangtze Craton have played an important role in the Tibetan Plateau growth and suggests that the Yangtze Craton might be reconstructed by ongoing continental collision.

KEYWORDS

adjoint tomography, lithospheric delamination, eastern Tibetan Plateau, mantle structure and dynamics, continent collision, asthenosphere upwelling

1 Introduction

The eastern Tibetan Plateau (Figure 1), the area of the latest growth of the plateau, is a preferable area to study when analyzing the geologic evolution of the Himalayan-Tibetan orogen. From south to north, the eastern Tibetan Plateau contains the eastern Himalayan syntaxis (EHS), the Songpan-Ganzi terrane (SPGZ) and the eastern Kunlun terrane (EKL). The EHS, where the Lhasa terrane rotated to a north-south trend during the Cenozoic era, was interpreted as a consequence of the convergence among the Indian Plate, Tibetan Plateau and the Burma block (Royden et al., 2008). To the east, the SPGZ is covered with thick and folding Triassic flysch complexes as well as widespread Mesozoic granitic plutons (Yuan et al., 2010). In the north, the Pre-Cenozoic EKL, Qilian orogen (QL) and Qaidam basin (QDB) form the northeast margin of the Tibetan Plateau and reveal significant crustal shortening of approximately 1,000–1,400 km since the Eocene (Yin and Harrison, 2000).

With the Alxa basin (AB), Ordos basin (OB), Sichuan basin (SCB), and Yangtze Craton separated by large-scale faults to the east (Tapponnier et al., 2001; Figure 1), the eastern margin

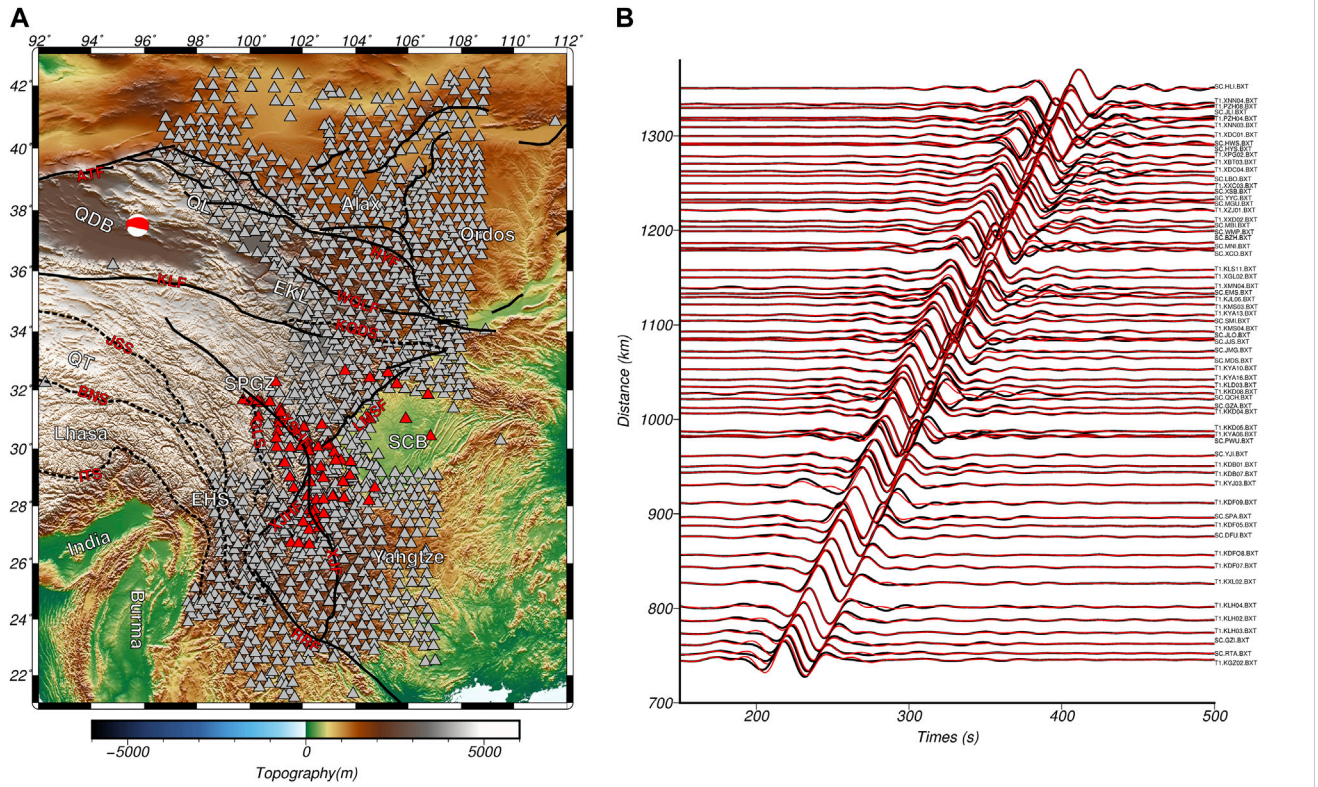

FIGURE 1
Topography, major tectonics, and seismic observations of the eastern Tibetan Plateau. **(A)** Black solid and dashed lines represent faults and suture zones obtained from the HimaTibetMap-1.1 dataset (Styron et al., 2010), respectively. Gray triangles represent the dense seismic array in the eastern Tibetan Plateau. Red triangles and beach balls represent seismic stations and earthquake event shown for waveform fitting. **(B)** Waveform fitting of the selected stations and event (earthquake ID 200811100122A, provided by https://www.globalcmt.org). Black lines denote the transverse component of the observed waveform and red lines denote the synthetics. ATF: Altyn Tagh fault, BNS: Bangong-Nujiang suture, EHS: Eastern Himalaya Syntaxis, EKL: eastern Kunlun terrane, GLS: Ganzi-Litang suture, HYF: Haiyuan fault, ITS: Indus-Tsangpo suture, JSS: Jinsha suture, KQDS: Kunlun-Qinglin-Dabie suture, LMSF: Longmenshan thrust belt, QDB: Qaidam basin, QL: Qilian orogen, QT: Qiangtang terrane, RRF: Red River fault, SCB: Sichuan basin, SPGZ: Songpan-Ganzi terrane, WQLF: West Qinglin fault, XJF: Xiaojiang fault, XJHF: Xiaojinhe fault, XSHF: Xianshuihe fault.

of the Tibetan Plateau currently suffers strong crustal deformation. Cenozoic volcanism and metallogenic deposits as well as large intraplate earthquakes are widely reported on the eastern margin of the Tibetan Plateau (Pei et al., 2019; Xu et al., 2021). In the past several decades, various studies have been conducted to determine how subsurface materials are exchanged between the eastern Tibetan Plateau and its surrounding regions (Tapponnier et al., 2001; Royden et al., 2008; Liu et al., 2014; Ye et al., 2015; Shen et al., 2017; Yang et al., 2020). However, the subsurface dynamics underneath the eastern Tibetan Plateau remain open to debate. For example, ductile flow-driven or rigid shear-induced processes need to be clarified. Moreover, a thorough understanding of the subsurface structure and mantle dynamics beneath the eastern margin of the Tibetan Plateau is necessary to further clarify the tectonic evolution of the plateau's expansion.

Many geophysical studies have been carried out within and around the eastern margin of the Tibetan Plateau to image the crust and the mantle structure. These research methods have included deep seismic sounding (Wang et al., 2007), magnetotelluric imaging (Bai et al., 2010), receiver function (Zhang et al., 2010), shear wave splitting (Chang et al., 2017) and seismic tomography (Yao et al., 2008; Lei and Zhao, 2016; Huang et al., 2019). However, even with these efforts, the principal dynamics of the eastern Tibetan Plateau in the Cenozoic era are still being debated. Models of the horizontal diffusion of the crust and mantle (Bai et al., 2010; Shen et al., 2017), the vertical upwelling of the asthenosphere (Bao et al., 2020) and the big mantle wedge (Lei and Zhao, 2016) have been postulated according to different geophysical observations. In other words, the deep structures beneath the eastern Tibetan Plateau have not been well resolved, either due to the irregular distribution of observations or the limited resolution of the tomographic methods.

In this study, we present 3-D seismic images of the entire upper mantle in the easternmost and northeastern Tibetan Plateau based on dense-array adjoint tomography. The combination of dense observations and accuracy tomographic techniques results in detailed images of the subsurface structure in the study region, which may help researchers reach better understanding of the geological evolution of the eastern Tibetan Plateau.

2 Data and methods

Extensive seismic observations have been performed on the eastern margin of the Tibetan Plateau to better understand the

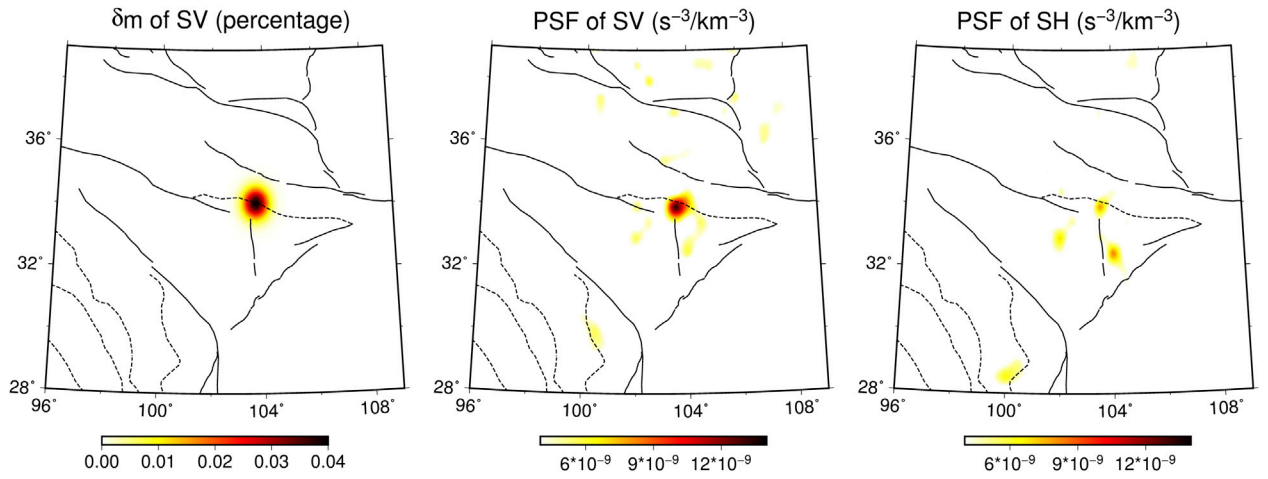

FIGURE 2
Point-spread function resolution test at the depth of 200 km beneath the eastern Tibetan Plateau. **(A)** The input Gaussian perturbation for V_{SV}. **(B)** The PSF output for V_{SV}. **(C)** The PSF output for V_{SH}.

lateral expansion of the Tibetan Plateau as well as the mechanisms of strong earthquakes. The large-scale broadband ChinArray project (triangles in Figure 1A), which has provided unprecedented data coverage with an average spacing of approximately 35 km, promotes the seismic study of the eastern Tibetan Plateau and has facilitated great progress (Zhang et al., 2017; Zhang et al., 2018). On the other hand, adjoint tomography (Tape et al., 2009), which provides high-accuracy in wavefield calculations and considers finite-frequency effects, has led to the new discovery of seismic features in heterogeneous regions.

Based on the large-scale ChinArray project and adjoint tomography methods, we built a seismic model of the Tibetan Plateau, named TP2019 (Xiao et al., 2020), that provides good illumination of the upper mantle of the eastern Tibetan Plateau. Benefitting from the inversion of multifrequency (from 12 to 100 s) body waves and surface waves recorded on three-component waveforms (Figure 1B), TP2019 reconstructed the subsurface structure with radial anisotropy, including the horizontally propagating with horizontally polarized shear velocity V_{SH} and the horizontally propagating with vertically polarized shear velocity V_{SV}. Spatial distribution of the misfit kernel shows good illumination of the upper mantle structure of the eastern Tibetan Plateau. In detail, point spread function resolution test suggest that an anomaly structure with radius of ~120 km could be resolved well by the current dataset (Figure 2). Details about the construction and assessment of the seismic model can be found in Xiao et al., 2020.

Here we provide a detailed interpretation of the upper mantle structures of the eastern margin of the Tibetan Plateau. As shear wave propagation is sensitive to mineral density, we present the structural features in terms of the isotropic shear wave velocity in the following section. The shear wave velocity is computed from the Voigt average (Babuska and Cara, 1991) of the elastic tensor over all angles in the radially anisotropic model as $V_S^2=2/3V_{SH}^2 + 1/3V_{SV}^2$.

3 Results

3.1 Shear wave velocity at upper mantle depths

In the shallow upper mantle (~100 km), the eastern Tibetan Plateau and surrounding basins (QDB, AB, OB, and SCB) as well as the Yangtze Craton are all imaged with high velocity, while the low-velocity imaging zones are located mostly in the easternmost Tibetan Plateau (Figure 3A). Receiver function studies have suggested that both the AB and OB are rigid blocks at the lithospheric scale (Shen et al., 2017), while the seismic velocity of the AB at a depth of 100 km is lower than those of the OB and SCB (Figure 3A). Vertical cross-sections of shear wave velocity from EHS to QDB (Figure 4A), AB (Figure 4B), OB (Figure 4C) and SCB (Figure 4D) show that high-velocity zones existed beneath these basins at depths shallower than ~200 km. However, the eastern margin of the SPGZ is depicted with significantly low-velocity anomalies at the shallow depths (Figures 3A, B; Figures 4C, D). Such low-velocity anomalies in the upper mantle show spatial consistency with the observed crustal low-velocity zones (Bao et al., 2020).

The strong contrast in velocity between the eastern margin of the Tibetan Plateau and the surrounding basins gradually becomes undetermined with depth, although low-velocity zones remain visible beneath the QL and the northeastern SPGZ (Figures 3C, D). Another distinctive feature is the vertical variation in the seismic velocity beneath the southeastern SPGZ. At the shallower upper mantle (~100 km), the southeastern SPGZ exhibits low-velocity features similar to those observed in the northeastern SPGZ (Figure 3A). However, the low velocity of the southeastern SPGZ suddenly converts to high velocity at a depth of 200 km, and these high velocities extend to deeper depths (Figures 3B–D). In addition, distinct high-velocity zones are observed beneath the EHS area (Figure 4). The high velocity of the EHS is visible in almost the entire upper mantle and is dominant in the lower upper mantle (Figures 3C, D).

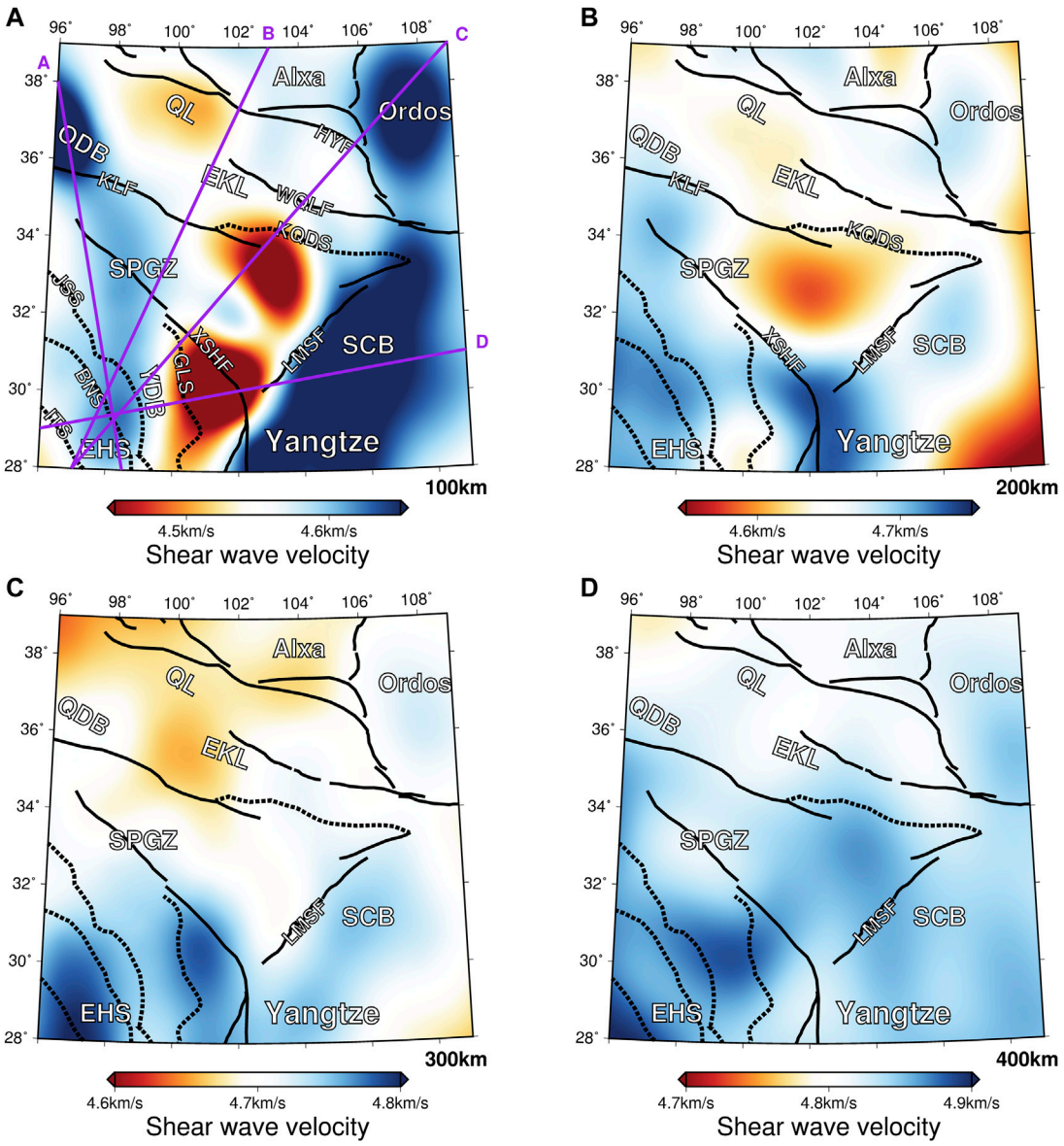

FIGURE 3
Shear velocity at the depth of 100 km **(A)**, 200 km **(B)**, 300 km **(C)** and 400 km **(D)** beneath the eastern Tibetan Plateau. The black lines represent sutures and faults, while the purple lines denote the locations of the vertical cross-sections in Figure 4.

3.2 Three-dimensional seismic structure of the upper mantle

Figure 5 shows the 3-D visualization of the shear velocity perturbation. High-velocity bodies are clearly present beneath the eastern Tibetan Plateau, OB and Yangtze Craton (Figures 5A, B). In the eastern Tibetan Plateau, the high-velocity body lies flat from the QDB to the SPGZ in the uppermost mantle and penetrates to great depths with a subvertical angle beneath the EHS (HV1, Figures 5B, C). Underneath the western SCB, the high-velocity body shows an oblique distribution toward the SPGZ, with a morphology similar to a subducting slab (HV2, Figures 5B, D). In contrary, low-velocity zones (LVZ) are present more or less beneath the eastern margin of the Tibetan Plateau, including a localized LVZ beneath the QL and a mushroom-shaped LVZ underneath the eastern SPGZ (Figures 5A, C). The mushroom-shaped LVZ is mainly distributed west of the Longmenshan thrust belt, originated from a depth of ~250 km.

4 Discussion

4.1 Subducted Indian slab beneath the eastern Himalayan syntaxis

Recent seismic studies suggest that subduction of the Indian plate might occur beneath the EHS (Li et al., 2008; Peng et al., 2015; Li and Song, 2018; Liu et al., 2019), although the manner of this subduction is controversial. Different hypotheses have been proposed: some authors

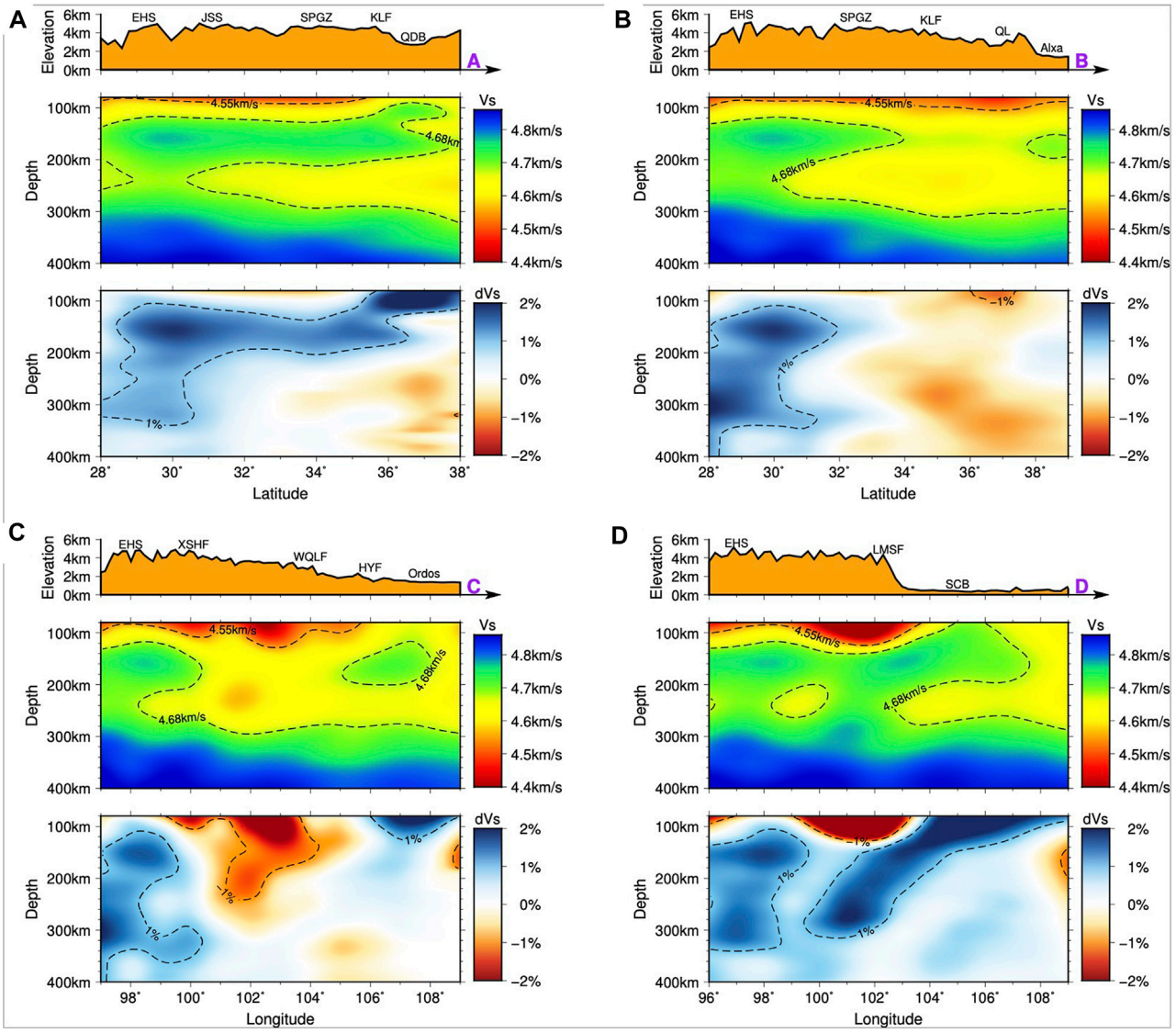

FIGURE 4
Vertical cross-sections of shear wave velocity of profile A **(A)**, B **(B)**, C **(C)** and D **(D)**. The locations of the cross-sections are shown in Figure 3A. The black solid and dotted lines represent the surface topography and contour of the seismic velocities, respectively. The perturbation is calculated relative to the 1-D mean velocity model of the research area.

have suggested continuous subduction (Li et al., 2008; Lei and Zhao, 2016), while others prefer slab tearing (Peng et al., 2015; Li and Song, 2018), slab breakoff (Zhang et al., 2017) or slab rollback (Liu et al., 2019).

In our tomographic images, the high-velocity body beneath the EHS (HV1) is visible throughout almost the entire upper mantle, showing a nearly vertical distribution (Figures 4, 5B). Furthermore, a high-velocity belt exists to the north of the EHS; this belt lies flat and is continuous from the EHS to the QDB above a depth of 200 km (Figure 4A). As the depth of the Lithosphere-Asthenosphere-Boundary varies within 200 km in the eastern Tibetan Plateau (Kumar et al., 2006), we suggest that this flat and high-velocity layer represents the base of the thickened lithosphere of the Tibetan Plateau. Therefore, the upper-mantle high-velocity anomalies of the eastern Tibetan Plateau can be divided into two parts: those beneath the EHS, which is a subducted slab of the Indian Plate, and those north of the EHS, which represents the thickened lithosphere of the Tibetan Plateau. These scenarios agree well with the hypotheses of the steep subduction or rollback of the Indian Plate beneath the EHS.

4.2 Lithospheric delamination and asthenosphere upwelling beneath the Western Yangtze Craton

Upper-mantle high-velocity anomalies beneath the easternmost Tibetan Plateau have been reported by recent seismic studies (Li et al., 2008; Lei and Zhao, 2016; Zhang et al., 2018; Huang et al., 2019; Wang et al., 2021). Nevertheless, the tectonic implications of such observations are far from explicit. Some studies have proposed that the high velocities in the mantle represent fragments of detached lithosphere (Huang et al.,

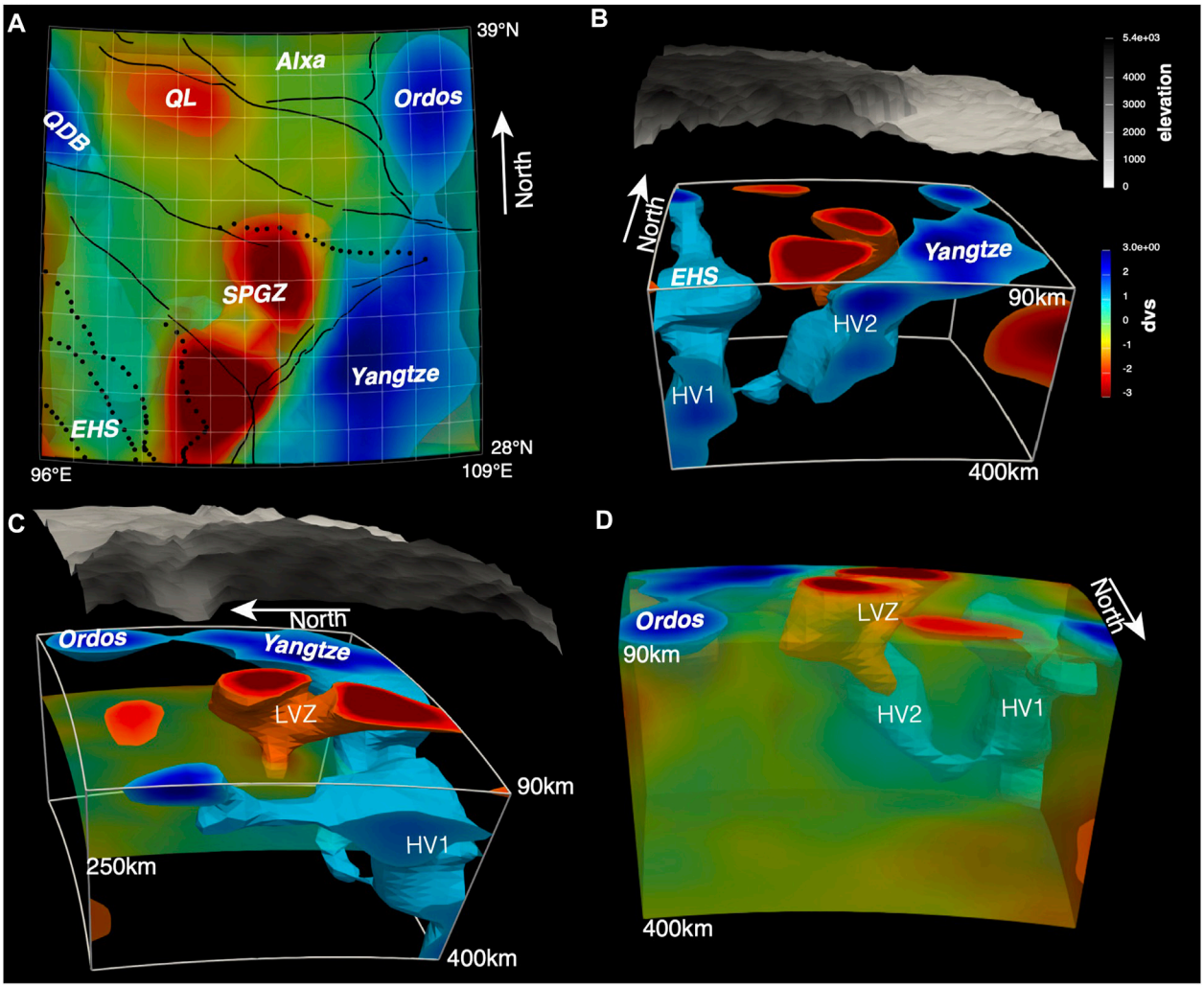

FIGURE 5
Mapview **(A)** and 3-D visualization of upper mantle shear velocity structures from south **(B)**, east **(C)** and north **(D)** direction. HV1: subvertical high velocity body beneath the EHS, HV2: oblique high velocity body beneath the western SCB, LVZ: low-velocity zones beneath the eastern margin of the Tibetan Plateau.

2019; Wang et al., 2021). However, the nature and process of lithospheric delamination are more rarely discussed.

With a west-dipping morphology similar to a slab, the high-velocity body beneath the western SCB (HV2) is apparently prone to subduction (Figure 5B). Although both the Cenozoic and Mesozoic westward subductions have been considered to have taken part in the evolution of the eastern margin of the Tibetan Plateau (Yuan et al., 2010; Ye et al., 2015), the driving forces of the westward subduction of the Yangtze Craton in the Cenozoic era as well as the preservation mechanism of the Mesozoic subduction are suspicious. On the other hand, the HV2 cannot be part of either the oceanic or continental Indian plate because of the robust westward dipping feature. Specifically, the HV2 is continuously connected to the high-velocity Yangtze Craton to the shallow depth, overlaid by a mushroom-shaped LVZ at the uppermost mantle between the EHS and the Yangtze Craton (Figures 4D, 5B). Therefore, it is reasonable to infer that the west-dipping HV2 is a part of the lithosphere that originates from the Yangtze Craton, i.e., the Yangtze Craton delaminates to the asthenosphere or even the uppermost lower mantle (Feng et al., 2022) in eastern Tibetan Plateau.

The morphology of continental delamination has been proposed to be highly similar to the subduction of a slab along a weak layer (Liu et al., 2018). As major consequences of delamination, regional uplift, increased heat flow, reduced seismic velocity and mafic volcanism have been widely reported on the eastern margin of the Tibetan Plateau and the western Yangtze Craton (Royden et al., 2008; Liu et al., 2014; Xu et al., 2021). Furthermore, the geodynamic modelling suggests an upwelling asthenosphere, which might be a response to the retreated subducting slab, could intrude the dense mantle lithosphere and eclogitized lower crust to delaminate during the continental collision (Gray and Pysklywec, 2012).

Continental lithosphere delamination (Bird, 1979) has been widely proposed in Tibetan Plateau from seismological, petrological, and geological observations (Tilmann et al., 2003; Chung et al., 2005). In western Yangtze, Pb-Sr-Nd isotopic analysis of petrological and geochemical studies (Tian et al., 2006; Hou et al., 2021) show that the potassic alkaline rocks and carbonate rocks (27–10 Ma) originated from an enriched EMI-EMII mantle source, indicating asthenosphere upwelling and partial melting of the lithospheric mantle as well as the timing of the lithospheric

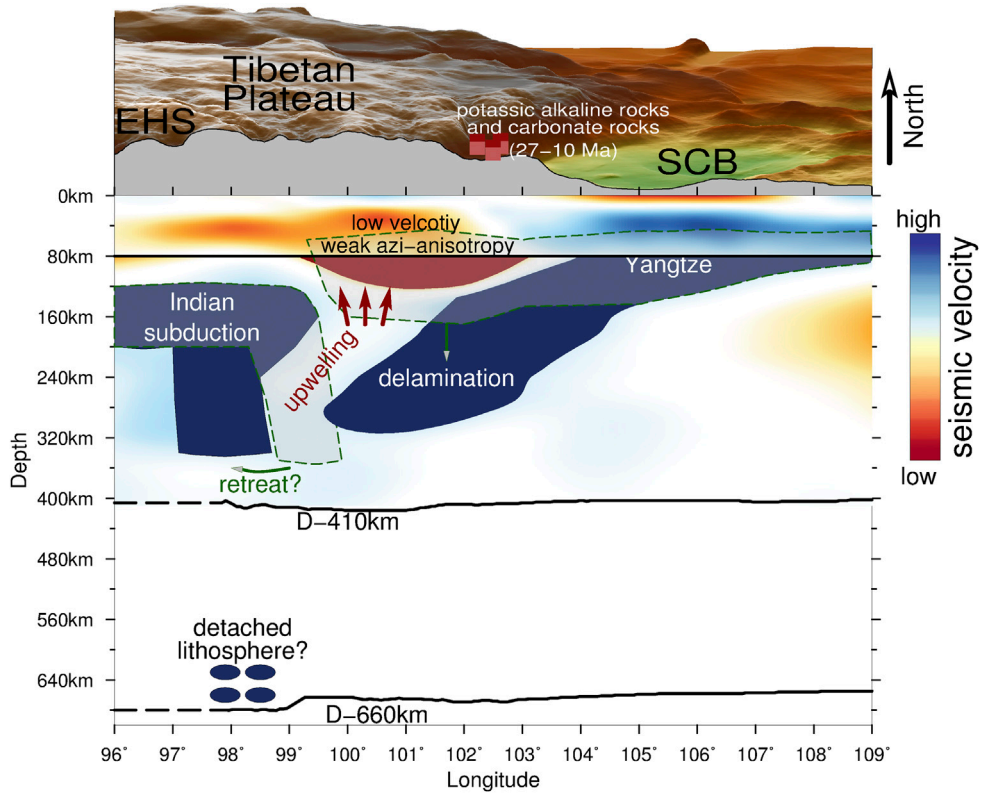

FIGURE 6
Deep tectonics of the eastern Tibetan Plateau. Seismic velocity perturbations in the upper mantle and crust are collected from this study and Bao et al., 2020, respectively. The depth of LAB, 410 and 660 km discontinuities are retrieved from Zhang et al., 2010 and Zhang et al., 2017. Red hexahedrons represent the western Sichuan potassic alkaline rocks and carbonate rocks (27–10 Ma), which are collected form Hou et al., 2021.

delamination. More recently, whole-rock geochemistry and olivine oxygen isotopes show that the Cenozoic mafic potassic lavas of the west Yangtze were derived from the lithospheric mantle at different depths and suggest a deep delaminated lithosphere was located beneath the southwestern Yangtze Craton, which is more fertile and denser than the shallow intact lithosphere (Wang et al., 2022). Such delamination could be caused by lithospheric thickening during the continental collision (Tilmann et al., 2003), or by slab retreat during continental/oceanic subduction (e.g., Gray and Pysklywec, 2012; Liu et al., 2018). Our results cannot distinguish an oceanic lithosphere from a continental lithosphere for HV1 which we crudely attribute to the Indian plate. However, several recent high-resolution seismic images in Myanmar suggest a continental lithosphere in the shallow ~100 km depth (Zheng et al., 2020) and an oceanic lithosphere continuously extending the mantle transition zone (Bai et al., 2020; Yang et al., 2022). Considering a nearly constant convergence of ~4–5 cm/yr between India and Asia, we thus deduce that the oceanic, rather than continental, slab subduction resulted in the delamination of the overlying lithosphere of Yangtze Craton in the Oligocene, probably due to the slab retreat of the Neo-Tethyan slab (Gray and Pysklywec, 2012; Liu et al., 2018).

Accordingly, we prefer to a continent delamination as the geological interpretation of the observed HV2 (Figure 6). The delamination of the western Yangtze was probably induced by the retreat of the subducting Indian Plate through the intrusion of the upwelling mantle materials. In this case, both the retreat of the Indian slab and lithospheric delamination of the western Yangtze might cause asthenosphere upwelling between the EHS and western Yangtze, which might be observed as the mushroom-shaped LVZ. The asthenosphere upwelling and lithospheric delamination could explain the lateral variation of the LAB depth (Zhang et al., 2010; Zhang and Deng, 2022), the localized crust-mantle low velocity and weak azimuthal anisotropy (Bao et al., 2020) as well as the depressed 660-km discontinuity observed beneath the eastern margin of the Tibetan Plateau (Figure 6). Consequently, convergence between the eastern Tibetan Plateau and western Yangtze Craton would be accommodated in the upper crust dominantly by pure-shear thickening above the zone of mantle upwelling, and the crustal deformation will be characterized by contraction at the plateau margins and extension within the plateau (Gray and Pysklywec, 2012).

5 Conclusion

To understand the subsurface process of the Tibetan Plateau's expansion, we present detailed seismic images of the upper mantle of the eastern Tibetan Plateau. Mushroom-shaped low-velocity zones are imaged at the uppermost mantle of the eastern margin of the Tibetan Plateau, showing evidence of asthenosphere upwelling. Two observed slab-like high-velocity bodies beneath the eastern Himalayan syntaxis and western Sichuan basin are attributed to the subduction of the

Indian plate and the delaminated lithosphere of the western Yangtze Craton, respectively. Our study shows that the mantle dynamics of the Yangtze Craton might have contributed notably to the growth at the eastern margin of the Tibetan Plateau.

Data availability statement

The original contributions presented in the study are included in the article/supplementary material, further inquiries can be directed to the corresponding author.

Author contributions

YG and XS designed the research, and ZX carried out the data collection and analysis. JY interpreted the tectonic setting of the region.

Funding

This research was supported by the National Natural Science Foundation of China Project (42104103) and China Postdoctoral Science Foundation (2020M672849). The waveform data were provided by China Seismic Array Data Management Center (http://doi.org/10.17616/R31NJMMK) at Institute of Geophysics, China Earthquake Administration(doi: 10.12001/ChinArray.Data), and the Data Management Center of IRIS with network code IU, IC, KN, KR, KZ, MY, TW, TM, etc. Figures were generated with GMT (Wessel et al., 2013) and IRIS EMC 3-D visualization tool. Seismic model of this study is available online (https://doi.org/10.17605/OSF.IO/KRA7Y).

Conflict of interest

The authors declare that the research was conducted in the absence of any commercial or financial relationships that could be construed as a potential conflict of interest.

Publisher's note

References

Babuska, V., and Cara, M. (1991). Seismic anisotropy in the Earth. *Mod. Approaches Geophys.* 10. doi:10.1007/978-94-011-3600-6

Bai, D., Unsworth, M. J., Meju, M. A., Ma, X., Teng, J., Kong, X., et al. (2010). Crustal deformation of the eastern Tibetan plateau revealed by magnetotelluric imaging. *Nat. Geosci.* 3 (5), 358–362. doi:10.1038/ngeo830

Bai, Y., Yuan, X., He, Y., Hou, G., Thant, M., Sein, K., et al. (2020). Mantle transition zone structure beneath Myanmar and its geodynamic implications. *Geochem. Geophys. Geosystems* 21 (12), e2020GC009262. doi:10.1029/2020GC009262

Bao, X., Song, X., Eaton, D. W., Xu, Y., and Chen, H. (2020). Episodic lithospheric deformation in eastern Tibet inferred from seismic anisotropy. *Geophys. Res. Lett.* 47, e2019GL085721. doi:10.1029/2019GL085721

Bird, P. (1979). Continental delamination and the Colorado plateau. *J. Geophys. Res. Solid Earth* 84 (B13), 7561–7571. doi:10.1029/JB084iB13p07561

Chang, L., Ding, Z., Wang, C., and Flesch, L. M. (2017). Vertical coherence of deformation in lithosphere in the NE margin of the Tibetan plateau using GPS and shear-wave splitting data. *Tectonophysics* 699, 93–101. doi:10.1016/j.tecto.2017.01.025

Chung, S.-L., Chu, M.-F., Zhang, Y., Xie, Y., Lo, C.-H., Lee, T.-Y., et al. (2005). Tibetan tectonic evolution inferred from spatial and temporal variations in post-collisional magmatism. *Earth-Science Rev.* 68 (3–4), 173–196. doi:10.1016/j.earscirev.2004.05.001

Feng, J., Yao, H., Chen, L., and Wang, W. (2022). Massive lithospheric delamination in southeastern Tibet facilitating continental extrusion. *Natl. Sci. Rev.* 9 (4), nwab174. doi:10.1093/nsr/nwab174

Gray, R., and Pysklywec, R. N. (2012). Geodynamic models of mature continental collision: Evolution of an orogen from lithospheric subduction to continental retreat/delamination: Geodynamics Mature Continental Collision. *J. Geophys. Res. Solid Earth* 117 (B3). doi:10.1029/2011JB008692

Hou, Z., Xu, B., Zheng, Y., Zheng, H., and Zhang, H. (2021). Mantle flow: The deep mechanism of large-scale growth in Tibetan Plateau. *Chin. Sci. Bull.* 66 (21), 2671–2690. doi:10.1360/TB-2020-0817

Huang, Z., Wang, L., Xu, M., Zhao, D., Mi, N., and Yu, D. (2019). P and S Wave tomography beneath the SE Tibetan Plateau: Evidence for lithospheric delamination. *J. Geophys. Res. Solid Earth* 124 (10), 10292–10308. doi:10.1029/2019JB017430

Kumar, P., Yuan, X., Kind, R., and Ni, J. (2006). Imaging the colliding Indian and asian lithospheric plates beneath tibet: Lithospheres beneath tibet. *J. Geophys. Res. Solid Earth* 111, B06308. doi:10.1029/2005JB003930

Lei, J., and Zhao, D. (2016). Teleseismic P-wave tomography and mantle dynamics beneath Eastern Tibet. *Geochem. Geophys. Geosystems* 17 (5), 1861–1884. doi:10.1002/2016GC006262

Li, C., van der Hilst, R. D., Meltzer, A. S., and Engdahl, E. R. (2008). Subduction of the Indian lithosphere beneath the Tibetan Plateau and Burma. *Earth Planet. Sci. Lett.* 274 (1–2), 157–168. doi:10.1016/j.epsl.2008.07.016

Li, J., and Song, X. (2018). Tearing of Indian mantle lithosphere from high-resolution seismic images and its implications for lithosphere coupling in southern Tibet. *Proc. Natl. Acad. Sci.* 115 (33), 8296–8300. doi:10.1073/pnas.1717258115

Liu, L., Gao, S. S., Liu, K. H., Li, S., Tong, S., and Kong, F. (2019). Toroidal mantle flow induced by slab subduction and rollback beneath the eastern himalayan syntaxis and adjacent areas. *Geophys. Res. Lett.* 46, 11080–11090. doi:10.1029/2019GL084961

Liu, L., Morgan, J. P., Xu, Y., and Menzies, M. (2018). Craton destruction 1: Cratonic keel delamination along a weak midlithospheric discontinuity layer. *J. Geophys. Res. Solid Earth* 123, 10,040. doi:10.1029/2017JB015372

Liu, Q. Y., van der Hilst, R. D., Li, Y., Yao, H. J., Chen, J. H., Guo, B., et al. (2014). Eastward expansion of the Tibetan Plateau by crustal flow and strain partitioning across faults. *Nat. Geosci.* 7 (5), 361–365. doi:10.1038/ngeo2130

Pei, S., Niu, F., Ben-Zion, Y., Sun, Q., Liu, Y., Xue, X., et al. (2019). Seismic velocity reduction and accelerated recovery due to earthquakes on the Longmenshan fault. *Nat. Geosci.* 12 (5), 387–392. doi:10.1038/s41561-019-0347-1

Peng, M., Jiang, M., Li, Z.-H., Xu, Z., Zhu, L., Chan, W., et al. (2015). Complex Indian subduction style with slab fragmentation beneath the Eastern Himalayan Syntaxis revealed by teleseismic P-wave tomography. *Tectonophysics* 667, 77–86. doi:10.1016/j.tecto.2015.11.012

Royden, L. H., Burchfiel, B. C., and van der Hilst, R. D. (2008). The geological evolution of the Tibetan Plateau. *Science* 321 (5892), 1054–1058. doi:10.1126/science.1155371

Shen, X., Liu, M., Gao, Y., Wang, W., Shi, Y., An, M., et al. (2017). Lithospheric structure across the northeastern margin of the Tibetan Plateau: Implications for the plateau's lateral growth. *Earth Planet. Sci. Lett.* 459, 80–92. doi:10.1016/j.epsl.2016.11.027

Styron, R., Taylor, M., and Okoronkwo, K. (2010). Database of active structures from the indo-asian collision. *Eos, Trans. Am. Geophys. Union* 91 (20), 181. doi:10.1029/2010EO200001

Tape, C., Liu, Q., Maggi, A., and Tromp, J. (2009). Adjoint tomography of the southern California crust. *Science* 325 (5943), 988–992. doi:10.1126/science.1175298

Tapponnier, P., Xu, Z., Francoise, R., Bertrand, M., Nicolas, A., Gérard, W., et al. (2001). Oblique stepwise rise and growth of the Tibet Plateau. *Science* 294 (5547), 1671–1677. doi:10.1126/science.105978

Tian, S., Hou, Z., Yuan, Z., Xie, Y., Fei, H., Yin, S., et al. (2006). Mantle source characteristics of magmatic carbonatites from the himalayan collision zone in Western sichuan, SW China: Evidence of Pb-Sr-Nd isotopes. *Acta Petrol. Sin.* 22 (3), 669–677. doi:10.18654/1000-0569/2006/022(03)-0669-77

Tilmann, F., and Ni, J.INDEPTH III Seismic Team (2003). Seismic imaging of the downwelling Indian lithosphere beneath central tibet. *Science* 300 (5624), 1424–1427. doi:10.1126/science.1082777

Wang, C.-Y., Han, W.-B., Wu, J.-P., Lou, H., and Chan, W. W. (2007). Crustal structure beneath the eastern margin of the Tibetan Plateau and its tectonic implications. *J. Geophys. Res.* 112 (B7), B07307. doi:10.1029/2005JB003873

Wang, J., Wang, Q., Xu, C.-B., Dan, W., Xiao, Z., Shu, C., et al. (2022). Cenozoic delamination of the southwestern Yangtze craton owing to densification during subduction and collision. *Geology* 50 (8), 912–917. doi:10.1130/G49732.1

Wang, W., Wu, J., and Hammond, J. O. S. (2021). Mantle dynamics beneath the Sichuan basin and eastern tibet from teleseismic tomography. *Tectonics* 40 (2). doi:10.1029/2020TC006319

Wessel, P., Smith, W. H. F., Scharroo, R., Luis, J., and Wobbe, F. (2013). Generic mapping tools: Improved version released. Eos, Transactions American Geophysical Union 94 (45), 409–410. doi:10.1002/2013EO450001

Xiao, Z., Fuji, N., Iidaka, T., Gao, Y., Sun, X., and Liu, Q. (2020). Seismic structure beneath the Tibetan Plateau from iterative finite-frequency tomography based on ChinArray: New insights into the Indo-Asian Collision. *J. Geophys. Res. Solid Earth* 125, e2019JB018344. doi:10.1029/2019JB018344

Xu, B., Hou, Z.-Q., Griffin, W. L., Zheng, Y.-C., Wang, T., Guo, Z., et al. (2021). Cenozoic lithospheric architecture and metallogenesis in Southeastern Tibet. *Earth-Science Rev.* 214, 103472. doi:10.1016/j.earscirev.2020.103472

Yang, J., Kaus, B. J. P., Li, Y., Leloup, P. H., Popov, A. A., Lu, G., et al. (2020). Lower crustal rheology controls the development of large offset strike-slip faults during the himalayan-Tibetan orogeny. *Geophys. Res. Lett.* 47 (18). doi:10.1029/2020GL089435

Yang, S., Liang, X., Jiang, M., Chen, L., He, Y., Thet Mon, C., et al. (2022). Slab remnants beneath the Myanmar terrane evidencing double subduction of the Neo-Tethyan Ocean. *Sci. Adv.* 8 (34), eabo1027. doi:10.1126/sciadv.abo1027

Yao, H., Beghein, C., and van der Hilst, R. D. (2008). Surface wave array tomography in SE tibet from ambient seismic noise and two-station analysis—II. Crustal and upper-mantle structure. *Geophys. J. Int.* 173 (1), 205–219. doi:10.1111/j.1365-246X.2007.03696.x

Ye, Z., Gao, R., Li, Q., Zhang, H., Shen, X., Liu, X., et al. (2015). Seismic evidence for the North China plate underthrusting beneath northeastern Tibet and its implications for plateau growth. *Earth Planet. Sci. Lett.* 426, 109–117. doi:10.1016/j.epsl.2015.06.024

Yin, A., and Harrison, T. M. (2000). Geologic evolution of the himalayan-Tibetan orogen. *Annu. Rev. Earth Planet. Sci.* 28 (1), 211–280. doi:10.1146/annurev.earth.28.1.211

Yuan, C., Zhou, M.-F., Sun, M., Zhao, Y., Wilde, S., Long, X., et al. (2010). Triassic granitoids in the eastern Songpan Ganzi Fold Belt, SW China: Magmatic response to geodynamics of the deep lithosphere. *Earth Planet. Sci. Lett.* 290 (3–4), 481–492. doi:10.1016/j.epsl.2010.01.005

Zhang, F., Wu, Q., Li, Y., Zhang, R., Sun, L., Pan, J., et al. (2018). Seismic tomography of eastern tibet: Implications for the Tibetan Plateau growth. *Tectonics* 37 (9), 2833–2847. doi:10.1029/2018TC004977

Zhang, R., Wu, Y., Gao, Z., Fu, Y. V., Sun, L., Wu, Q., et al. (2017). Upper mantle discontinuity structure beneath eastern and southeastern Tibet: New constraints on the Tengchong intraplate volcano and signatures of detached lithosphere under the Western Yangtze Craton. *J. Geophys. Res. Solid Earth* 122 (2), 1367–1380. doi:10.1002/2016JB013551

Zhang, Z., and Deng, Y. (2022). A generalized strategy from S-wave receiver functions reveals distinct lateral variations of lithospheric thickness in southeastern tibet. *Geochem. Geophys. Geosystems* 23 (11). doi:10.1029/2022GC010619

Zhang, Z., Yuan, X., Chen, Y., Tian, X., Kind, R., Li, X., et al. (2010). Seismic signature of the collision between the east Tibetan escape flow and the Sichuan Basin. *Earth Planet. Sci. Lett.* 292 (3–4), 254–264. doi:10.1016/j.epsl.2010.01.046

Zheng, T., He, Y., Ding, L., Jiang, M., Ai, Y., Mon, C. T., et al. (2020). Direct structural evidence of Indian continental subduction beneath Myanmar. *Nat. Commun.* 11 (1), 1944. doi:10.1038/s41467-020-15746-3